Correlation between the optical loss and crystalline quality in erbium-doped GaN optical waveguides

I-Wen Feng,[1] Weiping Zhao,[1] Jing Li,[1] Jingyu Lin,[1] Hongxing Jiang,[1,*] and John Zavada[2]

[1]Department of Electrical and Computer Engineering, Texas Tech University, Lubbock, Texas 79409, USA

[2]Department of Electrical and Computer Engineering, Polytechnic Institute of New York University, Brooklyn, New York 11201, USA

*Corresponding author: hx.jiang@ttu.edu

Erbium-doped GaN (GaN:Er) epilayers were synthesized by metal organic chemical vapor deposition. GaN:Er waveguides were fabricated based on four different GaN:Er layer structures: GaN:Er/GaN/Al$_2$O$_3$, GaN:Er/GaN/AlN/Al$_2$O$_3$, GaN:Er/GaN/Al$_{0.75}$Ga$_{0.25}$N/AlN/Al$_2$O$_3$, and GaN/GaN:Er/GaN/Al$_2$O$_3$. Optical loss at 1.54 μm in these waveguide structures has been measured. It was found that the optical attenuation coefficient of the GaN:Er waveguide increases almost linearly with the GaN (002) x-ray rocking curve linewidth. The lowest measured loss was ~6 dB/cm. © 2013 Optical Society of America

OCIS codes: (160.5690) Rare-earth-doped materials; (230.7370) Waveguides.
http://dx.doi.org/10.1364/AO.52.005426

1. Introduction

Trivalent Er atoms (Er^{3+}) give 1.54 μm emission that coincides with the minimal optical attenuation window of silica fibers, and hence Er-doped dielectric materials and semiconductors have been intensively researched for applications in optical communications, such as optical amplifiers, infrared emitters, and other optoelectronic devices [1–3]. In particular, the capability of an electrical excitation makes Er-doped semiconductors promising candidates for integration into compact modules with optical switches, wavelength-division multiplexing, and other photonic devices [4–6]. So far, silica and indium phosphide (InP) are the two dominant materials used to make integrated optical circuits. Although silica-based optical components have low propagation loss and high coupling efficiency with optical fibers because of the matched refractive index ($n = 1.5$), silica has a limited potential for realizing active functions due to its passive nature. On the other hand, InP-based optical devices are highly temperature sensitive and suffer from high fiber coupling loss due to interface reflection (index mismatch) and waveguide size mismatch. The refractive index of GaN decreases with wavelength and reaches to approximately 2.31 in the 1550 nm wavelength window [7]. This provides a much better refractive index match with optical fibers than InP does. Furthermore, among various semiconductors, III-nitrides have the advantage in terms of better thermal stability due to their wide energy bandgap and high thermal conductivity [8–11], and hence have been considered as promising hosts for Er doping for the fabrication of the robust and compact new generation of optoelectronic devices.

One of the potential applications of Er-doped III-nitride materials is to serve as optical waveguides and even Er-doped waveguide amplifiers (EDWAs) [1]. The optical gain (G) determines the performance of EDWAs and can be expressed as the following [12]:

$$G = \Gamma(g - \alpha)L, \qquad (1)$$

where g, Γ, α, and L refer to the gain coefficient, confinement factor, optical attenuation coefficient, and length of the waveguide, respectively. That is, a greater optical gain of EDWA can be realized through the design of a cavity that gives an enhanced confinement factor, an increase in the length of the waveguide, an improvement in the stimulated 1.54 μm emission of the active Er-doped materials, and a reduction in the optical loss. In this work, we determined the correlation between the crystalline quality and the optical loss in Er-doped GaN (GaN:Er) based optical waveguides, which may offer a guide for future designs and applications in EDWA based on Er-doped III-nitride materials.

2. Experimental Details

GaN:Er epilayers were synthesized using metal organic chemical vapor deposition (MOCVD) with *in situ* Er doping, where trimethylgallium (TMGa), tris-isopropylcyclopentadienyl-erbium (TRIPEr), and ammonia (NH_3) were used as the group-III, Er dopant, and group-V precursors, respectively. Four different GaN:Er samples with a similar Er concentration (N_{Er}) of about 2×10^{-20} cm^{-3} were selected in this study, and their layer structures are shown in Fig. 1: A1 (GaN:Er/GaN/AlN/Al$_2$O$_3$), A2 (GaN:Er/GaN/Al$_{0.75}$Ga$_{0.25}$N/AlN/Al$_2$O$_3$), A3 (GaN/GaN:Er/GaN/Al$_2$O$_3$), and A4 (GaN:Er/GaN/Al$_2$O$_3$). Here, we estimated N_{Er} based on the molar flow rate ratio of TRIPEr to TMGa precursors using a GaN:Er reference sample in which N_{Er} was calibrated by secondary ion mass spectrometry performed by Evans Analytical Group. The Al$_2$O$_3$ substrates used were epi-ready wafers with the orientation of C off M 0.2 ± 0.1 deg. The adoption of Al-rich AlGaN or AlN templates as the cladding layers of GaN:Er waveguides offers a larger contrast of the refractive index between the core and cladding layers leading
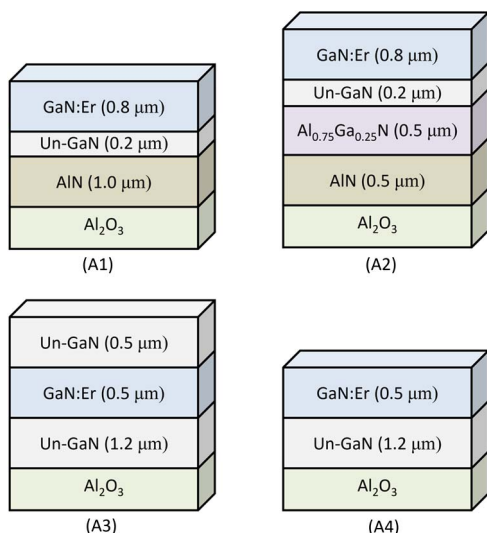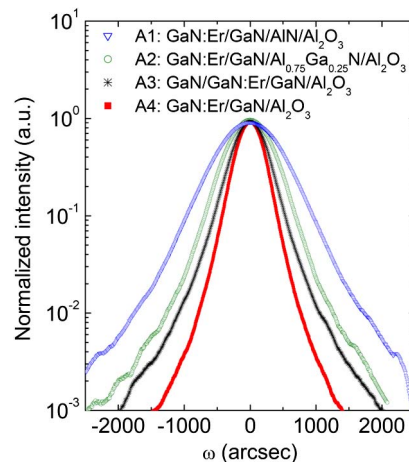

Fig. 2. GaN (002) XRD rocking curves measured from four different GaN:Er samples: A1 (GaN:Er/GaN/AlN/Al$_2$O$_3$), A2 (GaN:Er/GaN/Al$_{0.75}$Ga$_{0.25}$N/AlN/Al$_2$O$_3$), A3 (GaN/GaN:Er/GaN/Al$_2$O$_3$), and A4 (GaN:Er/GaN/Al$_2$O$_3$).

to a better optical confinement factor—where the confinement factor on active GaN:Er layers increases from 10% (A4) to 82% (A1) modeled with the infinite slab waveguides [7,13]—and the strain induced by the lattice mismatch between GaN:Er and Al-rich AlGaN or AlN templates may also provide an enhanced 1.54 μm emission [14]. However, the large difference in the lattice constants also brings about a relatively inferior crystalline quality of GaN:Er epilayers, where the in-plane lattice constants of GaN and AlN are 3.189 and 3.112 Å, respectively [15]. Here, we used x-ray diffraction (XRD) measurement to calibrate the crystalline qualities of these GaN:Er samples. As shown in Fig. 2, the full-width at half-maximum (FWHM) of GaN (002) XRD rocking curves (ω-scan) increases with the incorporation of the underneath Al-rich AlGaN or AlN templates. Our undoped GaN epilayers grown on sapphire synthesized with the same MOCVD system typically have a FHWM ~360 arcsec. We believe that the strain accumulated due to the difference in Ga-N and Er-N bonds induces a certain number of crystalline imperfections and hence may lead to a broadening in FWHM for our GaN:Er samples [16]. Also listed in Table 1 are the parameters of these four different GaN:Er samples including the surface morphology and the optical and crystalline properties.

GaN:Er waveguide mesas were patterned using chloride-based inductively coupled plasma (ICP) etching, followed by the deposition of a ~250 nm thick SiO$_2$ layer using plasma-enhanced chemical vapor deposition. The function of the capped SiO$_2$ layer is to minimize the optical loss caused by the surface roughness caused by waveguide processing [17,18]. Four GaN:Er waveguides have similar dimensional configurations with height $h \sim (0.9 \pm 0.1$ μm) and width $w \sim (12 \pm 1$ μm). The atomic force microscopy (AFM) image and schematic diagram of a GaN:Er waveguide based on (A4) GaN:Er/GaN/Al$_2$O$_3$ are shown in Fig. 3. Also depicted in Fig. 3 is the

Fig. 1. Schematic structure diagrams of four different GaN:Er samples: A1 (GaN:Er/GaN/AlN/Al$_2$O$_3$), A2 (GaN:Er/GaN/Al$_{0.75}$Ga$_{0.25}$N/AlN/Al$_2$O$_3$), A3 (GaN/GaN:Er/GaN/Al$_2$O$_3$), and A4 (GaN:Er/GaN/Al$_2$O$_3$).

Table 1. Parameters of Four Different GaN:Er Samples[a]

Sample Label	Layer Structure	FWHM (arcsec)	RMS (nm)	I_{emi} (a.u.)
A1	GaN:Er/GaN/AlN/Al$_2$O$_3$	940	4	29
A2	GaN:Er/GaN/Al$_{0.75}$Ga$_{0.25}$N/AlN/Al$_2$O$_3$	650	7	21
A3	GaN/GaN:Er/GaN/Al$_2$O$_3$	530	4	10
A4	GaN:Er/GaN/Al$_2$O$_3$	430	5	13

[a]FWHM of GaN (002) XRD rocking curves in ω-scan, root mean square (RMS) roughness in 10 μm × 10 μm AFM scan, and relative intensity of the 1.54 μm emission (I_{emi}) probed at the sample surface.
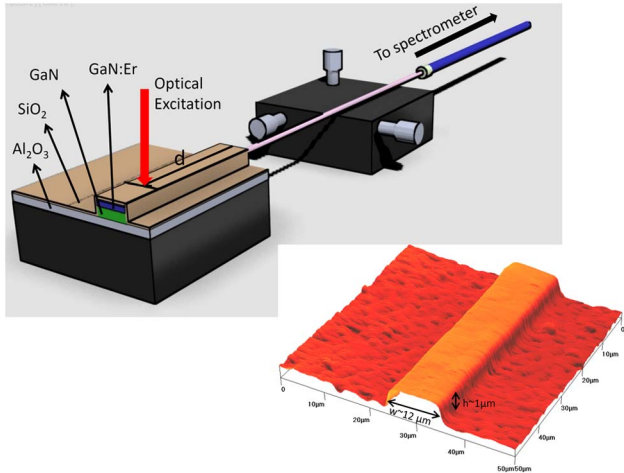

Fig. 3. Schematic diagram of the optical attenuation measurement setup and an AFM image of the GaN:Er waveguide fabricated based on sample A4 (GaN:Er/GaN/Al$_2$O$_3$) with waveguide width $w \sim 12$ μm and height $h \sim 1$ μm.

setup of the optical attenuation measurement used in this work. An above bandgap excitation with $\lambda_{exc} = 350$ nm was used as an optical excitation light source for generation of the 1.54 μm emission of the GaN:Er waveguides. The 1.54 μm emission was then collected from the detection end of the GaN:Er waveguides using an optical fiber connected to a thermoelectric-cooled InGaAs infrared spectrometer (Bayspec). As the excitation spot was moved farther away from the detection end of the GaN:Er waveguide with a separation distance (d), the detected intensity of the 1.54 μm emission decreased with d as described in the following equation [19]:

$$I(d) = I(0) \exp(-\alpha d), \qquad (2)$$

where $I(0)$ and $I(d)$ refer to the intensities of the 1.54 μm emission at the excitation spot and a distance d away from the excitation spot, respectively.

3. Results and Discussion

Shown in Fig. 4 are the results of the optical attenuation measurements of the GaN:Er waveguides fabricated based on these four different GaN:Er structures: A1 (GaN:Er/GaN/AlN/Al$_2$O$_3$), A2 (GaN:Er/GaN/Al$_{0.75}$Ga$_{0.25}$N/AlN/Al$_2$O$_3$), A3 (GaN/GaN:Er/GaN/Al$_2$O$_3$), and A4 (GaN:Er/GaN/Al$_2$O$_3$). With an increase in FWHM, the negative slope of $I(d)$ versus d becomes steeper. That is, the optical

loss in GaN:Er waveguides fabricated from samples A1 (GaN:Er/GaN/AlN/Al$_2$O$_3$) and A2 (GaN:Er/GaN/Al$_{0.75}$Ga$_{0.25}$N/AlN/Al$_2$O$_3$) becomes more significant. The effective optical attenuation coefficients of the four GaN:Er waveguides could be estimated from Fig. 4 using Eq. (2), and they were observed to increase in the sequence with samples A4, A3, A2, and A1.

One possible cause of the optical loss in optical waveguides is the scattering loss caused by the surface roughness of GaN:Er epilayers. However, we did not observe an obvious correlation between the measured optical attenuation and the surface roughness of GaN:Er epilayers. Instead, the effective optical attenuation coefficients of these GaN:Er waveguides are shown to depend on the linewidth of GaN (002) XRD rocking curves in ω-scan. As shown in Fig. 5, the optical attenuation coefficient increases almost linearly with an increase of the FWHM of GaN (002) XRD rocking curves. An increase in the FWHM of the XRD rocking curve indicates the presence of a larger number of crystalline dislocations in GaN:Er epilayers grown on Al-rich AlGaN or AlN templates [20]. These embedded crystalline dislocations may play a role as light scattering centers, which explain the correlation between the XRD linewidth and optical loss. The optical attenuation
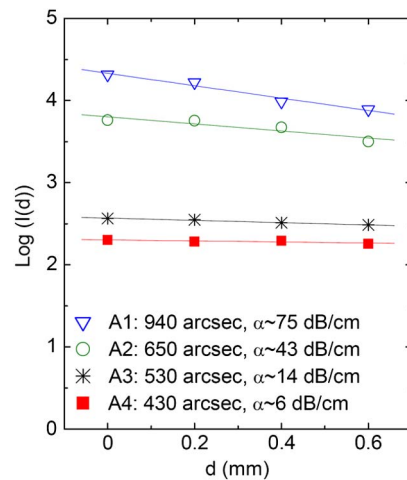

Fig. 4. Optical attenuation measurement results obtained from GaN:Er waveguides fabricated based on four different structures: A1 (GaN:Er/GaN/AlN/Al$_2$O$_3$), A2 (GaN:Er/GaN/Al$_{0.75}$Ga$_{0.25}$N/AlN/Al$_2$O$_3$), A3 (GaN/GaN:Er/GaN/Al$_2$O$_3$), and A4 (GaN:Er/GaN/Al$_2$O$_3$). The solid lines are the least-squares fit of data using Eq. (2).
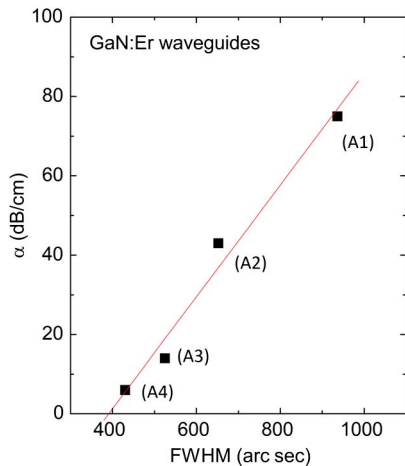
Fig. 5. Optical attenuation coefficient of GaN:Er waveguides as a function of the GaN (002) XRD rocking curve linewidth measured from four different structures: A1 (GaN:Er/GaN/AlN/Al$_2$O$_3$), A2 (GaN:Er/GaN/Al$_{0.75}$Ga$_{0.25}$N/AlN/Al$_2$O$_3$), A3 (GaN/GaN:Er/GaN/Al$_2$O$_3$), and A4 (GaN:Er/GaN/Al$_2$O$_3$).

coefficient observed in sample A4 is comparable to the value observed in Er-doped glass waveguides [21].

4. Summary and Conclusions

In summary, GaN:Er optical waveguides operating at 1.54 μm have been fabricated from different layer structures. Although GaN:Er epilayers grown on Al-rich AlGaN or AlN templates have advantages over the ones grown on GaN templates in terms of the optical confinement factor and 1.54 μm emission intensity, the lattice mismatch between GaN:Er epilayers and Al-rich AlGaN or AlN templates leads to higher crystalline dislocation densities in GaN:Er epilayers. This in turn leads to higher optical loss in the GaN:Er waveguides. Our previous results indicate that the absorption cross section of Er^{3+} in GaN is about $\sigma_a \sim 10^{-20}$ cm^2 at $\lambda = 1.54$ μm [22]. This implies that the optical absorption attenuation due to the presence of Er with N$_{Er} \sim 2 \times 10^{20}$ cm^{-3} is about ~3 dB/cm.

References

1. D. R. Zimmerman and L. H. Spiekman, "Amplifiers for the masses: EDFA, EDWA, and SOA amplets for metro and access applications," J. Lightwave Technol. **22**, 63–70 (2004).

2. J. D. B. Bradley and M. Pollnau, "Erbium-doped integrated waveguide amplifiers and lasers," Laser Photon. Rev. **5**, 368–403 (2011).

3. A. R. Peaker, "Erbium in semiconductors: where are we coming from; where are we going?," MRS Proc. **866**, 3–12 (2005).

4. R. Dahal, J. Y. Lin, H. X. Jiang, and J. M. Zavada, "Near infrared photonic devices based on Er-doped GaN and InGaN," Opt. Mater. **33**, 1066–1070 (2011).

5. R. Dahal, C. Ugolini, J. Y. Lin, H. X. Jiang, and J. M. Zavada, "1.54 μm emitters based on erbium doped InGaN p-i-n junctions," Appl. Phys. Lett. **97**, 141109 (2010).

6. A. Koizumi, Y. Fujiwara, A. Urakami, K. Inoue, T. Yoshikane, and Y. Takeda, "Effects of active layer thickness on Er excitation cross section in GaInP/GaAs: Er, O/GaInP double heterostructure light-emitting diodes," Phys. B **340**, 309–314 (2003).

7. R. Q. Hui, Y. T. Wan, J. Li, S. X. Jin, J. Y. Lin, and H. X. Jiang, "III-nitride-based planar lightwave circuits for long wavelength optical communications," IEEE J. Quantum Electron. **41**, 100–110 (2005).

8. A. J. Neuhalfen and B. W. Wessels, "Thermal quenching of Er^{3+} related luminescence in In$_{1-X}$Ga$_X$P," Appl. Phys. Lett. **60**, 2657–2659 (1992).

9. X. Z. Wang and B. W. Wessels, "Thermal quenching properties of Er doped GaP," Appl. Phys. Lett. **64**, 1537–1539 (1994).

10. C. Ugolini, N. Nepal, J. Y. Lin, H. X. Jiang, and J. M. Zavada, "Erbium-doped GaN epilayers synthesized by metal-organic chemical vapor deposition," Appl. Phys. Lett. **89**, 151903 (2006).

11. J. Zavada and D. Zhang, "Luminescence properties of erbium in III–V compound semiconductors," Solid-State Electron. **38**, 1285–1293 (1995).

12. K. Gerd, *Optical Fiber Communications* (McGraw-Hill, 1998).

13. C. R. Pollock, *Fundamentals of Optoelectronics* (Irwin, 1995).

14. I. W. Feng, J. Li, A. Sedhain, J. Y. Lin, H. X. Jiang, and J. Zavada, "Enhancing erbium emission by strain engineering in GaN heteroepitaxial layers," Appl. Phys. Lett. **96**, 031908 (2010).

15. W. G. Perry, T. Zheleva, M. D. Bremser, R. F. Davis, W. Shan, and J. J. Song, "Correlation of biaxial strains, bound exciton energies, and defect microstructures in GaN films grown on AlN/6H-SiC(0001) substrates," J. Electron. Mater. **26**, 224–231 (1997).

16. A T. Wojtowicz, P. Ruterana, N. Rousseau, O. Briot, S. Dalmasso, R. W. Martin, and K. P. O'Donnell, "The microstructure of Er MBE doped GaN," Mater. Sci. Eng. B **105**, 114–117 (2003).

17. F. P. Payne and J. P. R. Lacey, "A theoretical-analysis of scattering loss from planar optical wave-guides," Opt. Quantum Electron. **26**, 977–986 (1994).

18. A. Kovalenko, V. Kurashov, and O. Matievosova, "Radiation losses in planar dielectric waveguide with random rough surface," in *2011 11th International Conference on Laser and Fiber-Optical Networks Modeling (LFNM)*, Kharkov, 2011, pp. 1–3.

19. R. Dahal, C. Ugolini, J. Y. Lin, H. X. Jiang, and J. M. Zavada, "Erbium-doped GaN optical amplifiers operating at 1.54 μm," Appl. Phys Lett. **95**, 111109 (2009).

20. M. Moram and M. Vickers, "X-ray diffraction of III-nitrides," Rep. Prog. Phys. **72**, 036502 (2009).

21. Y. Yan, A. J. Faber, H. De Waal, P. G. Kik, and A. Polman, "Erbium-doped phosphate glass waveguide on silicon with 4.1 dB/cm gain at 1.535 μm," Appl. Phys. Lett. **71**, 2922–2924 (1997).

22. Q. Wang, R. Dahal, I. W. Feng, J. Y. Lin, H. X. Jiang, and R. Hui, "Emission and absorption cross-sections of an Er:GaN waveguide prepared with metal organic chemical vapor deposition," Appl. Phys. Lett. **99**, 121106 (2011).